Indian Journal of Natural Products and Resources
Vol. 15(3), September 2024, pp. 364-380
DOI: 10.56042/ijnpr.v15i3.4938

# Flavonoids from *Zingiber roseum* rhizome modulate potential diabetic targets: Computational approach

Muhammed Amanat[1], Md. Sorforajur Rahman[2] and Randhir Singh[1]*

[1]Department of Pharmacology, Central University of Punjab, Ghudda, Bathinda 151401, India

[2]Department of Pharmacy, Noakhali Science and Technology University, Sonapur, Noakhali 3814, Bangladesh

*Received 16 August 2023; revised received 08 May 2024; accepted 13 May 2024*

Despite the availability of several antidiabetic drugs, it is still an uphill task for the medical fraternity to find an appropriate treatment to control diabetes without developing any adverse effects. Consequently, there is a growing need for safer, natural anti-diabetic medications. Traditionally, herbal remedies have been heavily relied on for diabetic care due to their rich reservoir of phyto-ingredients, especially flavonoids. Nevertheless, the complexity of herbal extracts poses a significant scientific challenge in isolating the precise therapeutic molecules accountable for their anti-diabetic properties. To address this matter, our study employed a computational approach to investigate the interaction of flavonoids extracted from *Zingiber roseum* rhizome (ZRR) with key targets implicated in diabetes, including α-amylase, α-glucosidase, pparγ, adiponectin, and glycogen synthase kinase-3β. The molecular docking simulations were performed using AutoDockPyRx, and the binding energies were calculated. Encouragingly, our findings revealed that the flavonoids rosmarinic acid and quercetin from ZRR showed highly favourable binding affinities with the selected targets, underscoring their potential as natural agents for combating diabetes. The primary objective of this computational investigation is to unveil novel flavonoids obtained from ZRR in the context of diabetes, shedding light on unexplored molecular pathways and potential therapeutic avenues.

**Keywords:** Anti-diabetic, Diabetes, PyRx, Quercetin, Rosmarinic acid, *Zingiber roseum*

**IPC code; Int. cl. (2021.01)**– A61K 36/00, A61K 36/906, A61K 125/00, A61P 3/10

## Introduction

Diabetes mellitus, commonly known as a chronic metabolic disorder, has plagued humankind for a long time, and its prevalence is generally acknowledged as high (4-5%) worldwide[1]. Nearly 415 million people have this significant endocrine disorder globally (almost 10%)[2,3]. By the end of 2030, this figure is expected to more than double[4]. In the case of diabetes, two main types have been recognised. Type 1 diabetes (insulin-dependent) results from autoimmune destruction of pancreatic β-cells, whereas type 2 diabetes (insulin-independent) is spurred on by obesity-induced β-cell malfunction[5]. After that, insulin therapy and oral hypoglycemic medications treat Type 1 and 2 diabetes[5]. Despite its usefulness in lowering blood sugar levels, insulin treatment comes with several drawbacks, including insulin resistance, nervosa, vascular dementia, fatty liver, limited shelf life, need for regular refrigeration, and catastrophic hypoglycemia[6-8]. As a result, diabetes adversely impacts an array of internal organs, including the liver, heart, kidney, muscle, pancreas, brain, and reproductive organs[9]. Consequently, gastrointestinal sensitivities, hypoglycemia shock, and alteration of liver and kidney functions are some of the undesirable side effects of oral anti-diabetic medication usage also (Biguanide and Sulphonylureas)[10]. As current treatments for diabetic mellitus have many limitations, researchers are always looking for more promising options from phytochemicals which is cost-effective and have fewer side effects.

In traditional medical practices, herbal plants play a vital function. Many people rely solely on plants to treat a wide range of health issues because of the difficulty of accessing modern treatment there. Traditional medicine has also been investigated to manage and cure diabetic diseases. Moreover, several studies have demonstrated plants with anti-diabetic activity[11-13]. Many bioactive chemicals in plants make it difficult to pinpoint the precise pharmacological agent and comprehend how they affect the complicated mechanisms underlying diabetes[14].

*Correspondent author
Email: randhir.singh@cup.edu.in
Mob.: +919896029234

The Zingiberaceae family comprises numerous valuable plants, including the therapeutic *Zingiber roseum*. This plant is a native perennial herb in Bangladesh and is often called "JangliAdrak"[15]. Traditionally, people have turned to this plant to alleviate symptoms, including coughing, high body temperature, skin disorders, liver infections, and stomach upset[15]. Scientific research has shown that the plant's rhizome contains antispasmodic and myorelaxant properties and is also rich in antioxidants[16]. Moreover, *Z. roseum* rhizome (ZRR) contains many active phytoconstituents showing numerous pharmacological activities[17-21].

Furthermore, seven flavonoids were identified using HPLC analysis in our prior research[15]. According to the literature, flavonoid has many biological activities, including antioxidant, anti-inflammatory, cardioprotective, anticancer, anti-diabetic, and so on[22-26]. In light of the prevailing understanding, the flavonoids catechin hydrate, epicatechin, rosmarinic acid, quercetin, and myricetin have been identified from ZRR so far. Therefore, we have meticulously curated these flavonoids to serve as focal points for our present investigation.

Nevertheless, to the best of our knowledge, no pharmacological study has been done to examine ZRR's anti-diabetic potential using a computational method. Recently, *in silico* docking and target-focused combinatorial chemistry have emerged as potent tools in drug discovery. Globally, scientists have conducted extensive studies on molecular targets for diabetes mellitus to discover novel anti-diabetic drugs. Adiponectin, α-amylase, α-glucosidase, peroxisome proliferator-activated receptor gamma (PPARγ), and glycogen synthase kinase-3β are some of the key targets[14].

Adiponectin is a protein hormone secreted by adipose tissue and is known for significantly affecting lipid and insulin metabolism[27]. Adiponectin has insulin-sensitizing effects, and its level is decreased in obesity and type 2 diabetes mellitus (T2DM)[28]. As a result, adiponectin is a promising target for anti-diabetic actions. The small intestine also contains an enzyme called alpha-glucosidase, which is essential for digesting carbohydrates. Its primary purpose is to convert complex carbohydrates into simple sugars that can be absorbed into circulation and utilised by the body for energy[29]. Thus, α-glucosidase is a crucial anti-diabetic target.

On the contrary, the principal function of α-amylase is to aid in the digestion of carbohydrates by breaking down the long chains of starch molecules into smaller, more easily digestible molecules[30]. The enzyme catalyses the hydrolysis of alpha-1,4-glycosidic bonds in starch, producing smaller fragments of glucose called dextrins[31,32]. α-amylase is involved in the initial step of carbohydrate breakdown, which takes place in the mouth and small intestine. In the mouth, the salivary glands secrete alpha-amylase to break down the starch in food as it is being chewed. In the small intestine, the pancreas secretes alpha-amylase into the duodenum to further break down the residual starch[33]. That is why α-amylase might be a therapeutic target against diabetes. Besides, one of the most critical transcriptional regulators of adipogenesis, insulin sensitivity, and glucose homeostasis is the peroxisome proliferator-activated receptor gamma[34,35]. Glycogen Synthase Kinase 3β (GSK-3β) is an enzyme that is crucial in regulating glucose metabolism and insulin signalling. GSK-3β is involved in inhibiting glycogen synthesis and glucose uptake and is also implicated in the regulation of insulin sensitivity. Several studies have shown that inhibiting GSK-3β can improve glucose metabolism and insulin sensitivity, making it a promising target for diabetes management. The present work was conducted from this perspective to find lead compounds from *Z. roseum* that might build a structurally robust contact with the active site of various anti-diabetic target proteins.

## Materials and Methods

### Ligands selection and preparation

Five flavonoids named catechin hydrate, epicatechin, rosmarinic acid, quercetin, and myricetin, previously identified by HPLC from a methanolic extract of *Z. roseum* were selected[15]. Using the PubChem database, we obtained the .sdf file formats for the 3D structures of all the chosen ligands and the reference drug for docking experiments. All compounds were augmented with hydrogen bonds, and the energy was decreased by using the CHARMM force field.

### Protein preparation

Protein Database Bank was queried for the three-dimensional structures of adiponectin (4DOU), alpha-amylase (1XH0), alpha-glucosidase (5NN5), peroxisome proliferator-activated receptor-γ (3GBK), and glycogen synthase kinase-3β (3F7Z)[14,36] (Fig. 1). After that, proteins were refined by removing extra chain components interacting with receptors and

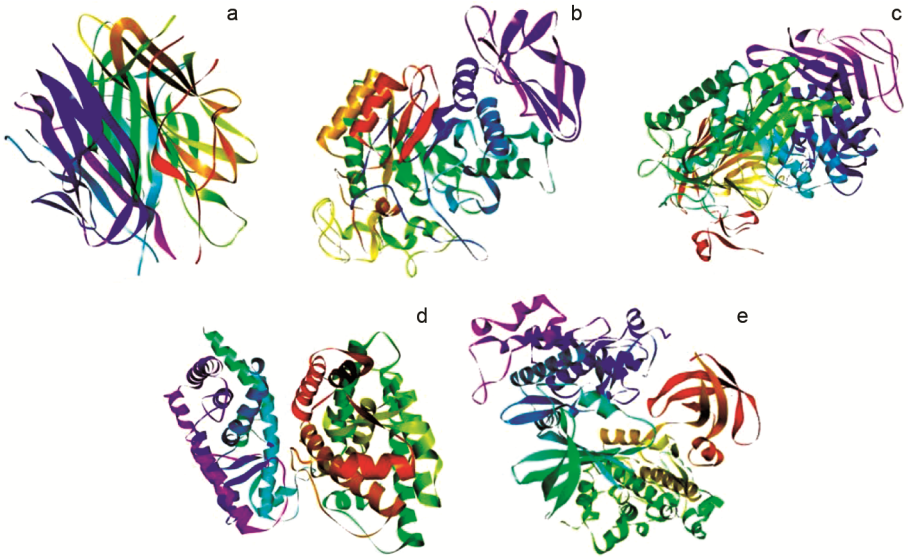


Fig. 1 — 3D structure of targeted proteins. a) Adiponectin; b) α-amylase; c) α glucosidase; d) PPARγ; and e) GSK-3β.

heteroatoms, ligands, water fragments, metal ions, etc. In addition, incorporating the necessary hydrogen atoms is a part of protein optimisation for successful docking. Overall optimisation was performed using UCSF Chimera Software Version 1.14; the resulting protein assembly was retrieved, analysed, and archived for further studies[15].

**Docking study and visualisation**

Virtual screening is mainly based on molecular docking. It seeks to anticipate the affinities and patterns of non-covalent interaction between two molecules. AutodockPyRx (0.8) was used to conduct the molecular docking study utilising a blind docking strategy[37,38]. Protein-ligand interactions were all mapped out by Discovery Studio users[15].

**ADMET and QSAR study**

ADME properties refer to a set of pharmacokinetic parameters that describe the absorption, distribution, metabolism, and excretion of drugs or other substances within the body. ADME properties play a critical role in drug discovery and development by providing necessary information on the pharmacokinetics and pharmacodynamics of a drug candidate. This information helps optimise drug formulations and dosing regimens and identify potential safety and toxicity concerns. On the contrary, QSAR (Quantitative Structure-Activity Relationship) properties are essential in drug discovery, chemical engineering, and material science. QSAR models use computational methods to relate the chemical structure of a molecule to its biological or chemical activity, allowing scientists to predict the activity of new compounds before synthesising them. Our current article evaluated the qualitative structure-activity relationship (QSAR) and ADMET data of five chosen ligands using molinspiration swiss ADME, pkCSM, and admetSAR2 sever[15,39].

**Biology activity prediction**

The projected biological activity profile of the five chemicals was summarized through the Prediction of Activity Spectra for Substance (PASS) program[15]. By analyzing the 2D or 3D chemical construction of biological substances, this online application may show over 4000 different forms of biological activity. Each compound's predicted information is shown as a Pa value (probability "to be active") and a Pi value (probability "to be inactive") for each activity. In the current investigation, more than 70% activity level is presumed to exist when the Pa value is more significant than 0.7 (pa > 0.7). The probability of finding a particular pharmacological activity in studies is more significant than Pi when Pa is greater than 0.7[40].

**Deformability, B-factor, and covariance computations**

To assess the mobility and stability of docked complexes, computational models of molecular dynamics (MD) were run using the iMODS database[41]. We performed deformability, B-factor, and covariance analyses on the bound complexes to identify residues that may still be fragile or deformed

following coarse-grained MD simulations. By default, the iMODS server received the docked PDB files[42].

**Root mean square fluctuation (RMSF) analysis**

Protein-ligand complexes were modeled using MD simulations through CABS-flex V 2.0[43]. CABS-flex was employed to determine the RMSF value. The simulation frequency was extended to 50 ns while all other parameters remained at standard settings. RMSFs were recorded using the default parameters based on the MD trajectory or NMR ensemble.

## Results and Discussion

**PASS online prediction of flavonoids identified in *Z. roseum* rhizomes extract**

The PASS web-based prediction engine examined the chosen chemicals' probable therapeutic activities and MAO. All compounds with Pa values greater than 0.07 were chosen for their significant biological activity. Possible biological characteristics and MAO for selected chemicals are listed in Table 1.

**Docking analysis**

The current study used the docking score to verify the likely binding affinity of medicines responsible for anti-diabetic benefits. In the PyRx program, the highest binding affinity score indicates the optimal docking relationship between protein and ligand; the binding score of all phytochemicals is represented in Tables 2-6.

Therefore, the compounds with the most docked protein targets are shown in Table 7. Compounds were chosen by comparing their docking score to that of the reference drug for each receptor; rosiglitazone was used as the reference drug for Adiponectin and PPAR-γ, acarbose was used as the reference drug for α-amylase and α-glucosidase, and metformin was used as the reference drug for GSK-3β. The data showed an excellent docking score against targeted receptors. It is worth mentioning that Rosmarinic acid and Quercetin bound to a maximum of five targets, making them the most successful compounds in binding scores (Table 7). However, Catechin hydrate and Epicatechin bind to four targets with the second-lowest affinity. Fig 2-6 depicts the molecular interactions between amino acid residues in the active regions of the targeted proteins and selected drugs. Therefore, docking interactions focused mainly on Hydrogen bonds[15].

**ADMET and QSAR analysis**

To ascertain the physicochemical interaction of a molecule with a specific target, it is necessary to analyse its absorption, distribution, metabolism, excretion, and toxicity (ADMET). Developing new medicines allows us to assess their viability as drug candidates, eventually identifying a novel lead molecule for a specific target domain[44]. After

Table 1 — Biological activity prediction of selected ligands regarding antidiabetic action

| Compound | Predicted MOA | Biological activity | |
|---|---|---|---|
| | | Pa | Pi |
| Catechin hydrate | ▪ Lipid peroxidase inhibitor | 0.888 | 0.003 |
| | ▪ Free radical scavenger | 0.842 | 0.002 |
| | ▪ Antioxidant | 0.810 | 0.003 |
| | ▪ JAK2 expression inhibitor | 0.785 | 0.009 |
| | ▪ Kidney function stimulant | 0.610 | 0.036 |
| | ▪ Antiinflammatory | 0.548 | 0.044 |
| | ▪ Antidiabetic | 0.355 | 0.058 |
| | ▪ Alpha glucosidase inhibitor | 0.300 | 0.003 |
| | ▪ Lipid metabolism regulator | 0.334 | 0.122 |
| | ▪ Aldose reductase inhibitor | 0.101 | 0.018 |
| Epicatechin | ▪ Lipid peroxidase inhibitor | 0.888 | 0.003 |
| | ▪ Free radical scavenger | 0.842 | 0.002 |
| | ▪ Antioxidant | 0.810 | 0.003 |
| | ▪ Peroxidase inhibitor | 0.721 | 0.010 |
| | ▪ Antihypercholesterolemic | 0.631 | 0.012 |
| | ▪ Kidney function stimulant | 0.610 | 0.036 |
| | ▪ Antiinflammatory | 0.548 | 0.044 |
| | ▪ TNF expression inhibitor | 0.517 | 0.026 |
| | ▪ Antidiabetic | 0.355 | 0.058 |
| | ▪ Alpha glucosidase inhibitor | 0.300 | 0.003 |
| Rosmarinic acid | ▪ Free radical scavenger | 0.745 | 0.003 |
| | ▪ TNF expression inhibitor | 0.744 | 0.005 |
| | ▪ Lipid peroxidase inhibitor | 0.719 | 0.005 |
| | ▪ Insulysin inhibitor | 0.625 | 0.020 |
| | ▪ Antidiabetic (type 2) | 0.609 | 0.006 |
| | ▪ Peroxisome proliferator-activated receptor gamma agonist | 0.571 | 0.003 |
| | ▪ Cholesterol antagonist | 0.570 | 0.024 |
| | ▪ Antioxidant | 0.539 | 0.005 |
| | ▪ Antiinflammatory | 0.496 | 0.008 |
| | ▪ Kidney function stimulant | 0.401 | 0.167 |
| Quercetin | ▪ Membrane integrity agonist | 0.973 | 0.002 |
| | ▪ Antioxidant | 0.872 | 0.003 |
| | ▪ Free radical scavenger | 0.811 | 0.003 |
| | ▪ Antiinflammatory | 0.689 | 0.017 |
| | ▪ Insulysin inhibitor | 0.645 | 0.017 |
| | ▪ Kidney function stimulant | 0.594 | 0.043 |
| | ▪ Aldose reductase inhibitor | 0.466 | 0.003 |
| | ▪ Alpha glucosidase inhibitor | 0.273 | 0.004 |
| | ▪ Antidiabetic symptomatic | 0.273 | 0.057 |
| | ▪ Antidiabetic | 0.195 | 0.019 |
| Myricetin | ▪ Antioxidant | 0,924 | 0.003 |
| | ▪ Lipid peroxidase inhibitor | 0,836 | 0.003 |
| | ▪ Free radical scavenger | 0,832 | 0.002 |
| | ▪ Antiinflammatory | 0,720 | 0.013 |
| | ▪ Kidney function stimulant | 0,620 | 0.032 |
| | ▪ Antihypercholesterolemic | 0,456 | 0.028 |

Table 2 — Molecular docking interactions of selected ligands adiponectin

| Name | Vina Score (kcal/mol) | Cavity volume (Å3) | Center (x, y, z) | Docking size (x, y, z) | Residues |
|---|---|---|---|---|---|
| Catechin hydrate | -6.7 | 967 | 5, -31, 23 | 21, 21, 21 | Chain A: LEU401 GLU402 THR403 TYR404 ILE407 PRO408 MET410 PRO411 ILE412 ARG413 THR415 VAL497 ASN504 LEU506 |
| Epicatechin | -7.0 | 961 | 5, -31, 23 | 21, 21, 21 | Chain A: LEU401 GLU402 THR403 TYR404 ILE407 PRO408 MET410 PRO411 ILE412 ARG413 THR415 VAL497 ASN504 LEU506 |
| Rosmarinic acid | -6.4 | 961 | 5, -31, 23 | 24, 24, 24 | Chain A: LEU401 GLU402 THR403 TYR404 ILE407 PRO408 MET410 PRO411 ILE412 ARG413 THR415 VAL497 ASN504 LEU506 |
| Quercetin | **-7.2** | 961 | 5, -31, 23 | 21, 21, 21 | Chain A: LEU401 GLU402 THR403 TYR404 ILE407 PRO408 MET410 PRO411 ILE412 ARG413 THR415 VAL497 ASN504 LEU506 |
| Myricetin | **-7.2** | 961 | 5, -31, 23 | 21, 21, 21 | Chain A: LEU401 GLU402 THR403 TYR404 ILE407 MET410 PRO411 ILE412 ARG413 THR415 VAL497 ASN504 LEU506 |
| Rosiglitazone | **-5.9** | 961 | 5, -31, 23 | 24, 24, 24 | Chain A: LEU401 GLU402 THR403 TYR404 ILE407 MET410 PRO411 ILE412 ARG413 PHE414 THR415 SER428 THR429 |

Table 3 — Molecular docking interactions of selected ligands against α-amylase

| Name | Vina Score | Cavity volume (Å3) | Center (x, y, z) | Docking size (x, y, z) | Residues |
|---|---|---|---|---|---|
| Catechin hydrate | **-9.1** | 541 | 9, 17, 43 | 21, 21, 21 | Chain A: TRP58 TRP59 TYR62 GLN63 HIS101 LEU162 THR163 LEU165 ARG195 ASP197 ALA198 GLU233 HIS299 ASP300 HIS305 |
| Epicatechin | -9.0 | 541 | 9, 17, 43 | 21, 21, 21 | Chain A: TRP58 TRP59 GLU60 TYR62 GLN63 HIS101 LEU162 THR163 LEU165 ARG195 ASP197 ALA198 GLU233 HIS299 ASP300 HIS305 |
| Rosmarinic Acid | -7.9 | 541 | 9, 17, 43 | 24, 24, 24 | Chain A: TRP58 TRP59 TYR62 GLN63 HIS101 LEU162 THR163 LEU165 ARG195 ASP197 ALA198 GLU233 ILE235 HIS299 ASP300 HIS305 GLY306 |
| Quercetin | -9.0 | 541 | 9, 17, 43 | 21, 21, 21 | Chain A: TRP58 TRP59 TYR62 GLN63 HIS101 LEU162 THR163 LEU165 ARG195 ASP197 ALA198 GLU233 HIS299 ASP300 HIS305 |
| Myricetin | -9.0 | 541 | 9, 17, 43 | 21, 21, 21 | Chain A: TRP58 TRP59 TYR62 GLN63 HIS101 LEU162 THR163 LEU165 ARG195 ASP197 ALA198 HIS201 GLU233 HIS299 ASP300 HIS305 |
| Acarbose | **-7.5** | 541 | 9, 17, 43 | 27, 27, 27 | Chain A: ILE51 TRP58 TRP59 TYR62 GLN63 HIS101 GLY104 ALA106 VAL107 TYR151 LEU162 THR163 GLY164 LEU165 ASP197 ALA198 LYS200 HIS201 GLU233 VAL234 ILE235 HIS299 ASP300 HIS305 |

Table 4 — Molecular docking interactions of selected ligands against α-glucosidase

| Name | Vina Score | Cavity volume (Å3) | Center (x, y, z) | Docking size (x, y, z) | Residues |
|---|---|---|---|---|---|
| Catechin hydrate | -7.2 | 1290 | 18, -25, 111 | 21, 21, 21 | Chain A: ARG696 LYS697 ALA698 THR700 LEU701 ASP774 LEU775 GLN776 THR777 VAL778 PRO779 ILE780 GLU781 THR813 ILE814 VAL816 |
| Epicatechin | -7.1 | 1290 | 18, -25, 111 | 21, 21, 21 | Chain A: ARG696 LYS697 THR700 LEU701 ASP774 LEU775 GLN776 VAL778 ILE780 GLU781 ILE814 VAL816 |
| Rosmarinic Acid | **-7.9** | 1290 | 18, -25, 111 | 24, 24, 24 | Chain A: GLN693 ARG696 LYS697 THR700 LEU701 ASP774 LEU775 GLN776 VAL778 PRO779 ILE780 GLU781 THR813 ILE814 ASN815 VAL816 |
| Quercetin | -7.1 | 1290 | 18, -25, 111 | 21, 21, 21 | Chain A: ARG696 LYS697 THR700 LEU701 ASP774 LEU775 GLN776 THR777 VAL778 ILE780 GLU781 ILE814 ASN815 VAL816 |
| Myricetin | -6.6 | 1290 | 18, -25, 111 | 21, 21, 21 | Chain A: ARG696 LYS697 THR700 LEU701 LEU775 GLN776 THR777 VAL778 ILE780 GLU781 ILE814 VAL816 |
| Acarbose | **-6.7** | 1290 | 18, -25, 111 | 27, 27, 27 | Chain A: LYS697 THR700 LEU701 ASP774 LEU775 GLN776 THR777 VAL778 PRO779 ILE780 VAL816 THR927 TYR928 SER929 THR932 VAL934 LEU935 ASP936 |

Table 5— Molecular docking interactions of selected ligands against PPARγ

| Name | Vina Score | Cavity volume (Å3) | Center (x, y, z) | Docking size (x, y, z) | Residues |
|---|---|---|---|---|---|
| Catechin hydrate | -8.0 | 13788 | 20, -6, 11 | 33, 35, 35 | Chain B: CYS285 GLN286 ARG288 SER289 HIS323 ILE326 TYR327 LEU330 MET334 VAL339 LEU340 ILE341 LEU353 PHE363 MET364 LYS367 HIS449 LEU453 LEU469 TYR473 |
| Epicatechin | -8.0 | 13788 | 20, -6, 11 | 33, 35, 35 | Chain A: HIS217 ASP220 SER221 LYS224 SER225 GLU298 LYS301 SER302Chain B: GLN294 THR297 LYS301 VAL315 LEU318 LYS319 LEU468 GLU471 ILE472 |
| Rosmarinic Acid | -8.2 | 13788 | 20, -6, 11 | 33, 35, 35 | Chain A: HIS217 ASP220 SER221 LYS224 SER225 GLU298 TYR299 LYS301 SER302Chain B: VAL293 GLN294 THR297 LYS301 GLN314 VAL315 LEU318 LYS319 VAL322 LEU468 GLU471 ILE472 |
| Quercetin | **-8.5** | 13788 | 20, -6, 11 | 33, 35, 35 | Chain B: CYS285 GLN286 ARG288 SER289 HIS323 ILE326 TYR327 LEU330 MET334 VAL339 LEU340 ILE341 PHE363 MET364 LYS367 HIS449 LEU453 LEU469 TYR473 |
| Myricetin | -7.5 | 13788 | 20, -6, 11 | 33, 35, 35 | Chain A: HIS217 LYS301 SER302 ILE303 PRO304 GLY305 PHE306 VAL307 ASN308Chain B: LYS224 SER225 PRO227 ARG288 GLU291 GLN294 GLU295 THR297 GLU298 GLU343 |
| Rosiglitazone | **-8.0** | 13788 | 20, -6, 11 | 33, 35, 35 | Chain B: PHE226 PRO227 LEU228 LEU270 ARG280 ILE281 GLY284 CYS285 ARG288 GLU295 MET329 LEU330 LEU333 VAL339 LEU340 ILE341 SER342 GLU343 GLY344 MET348 LEU353 |

Table 6 — Molecular docking interactions of selected ligands against GSK-3β

| Name | Vina Score | Cavity volume (Å3) | Center (x, y, z) | Docking size (x, y, z) | Contact Residues |
|---|---|---|---|---|---|
| Catechin hydrate | -5.9 | 1293 | -29, 20, 21 | 29, 21, 21 | Chain B: TYR140 ALA143 ARG144 SER147 LYS183 PRO184 GLN185 SER219 TYR221 TYR222 GLU249 GLY253 GLN254 PRO255 |
| Epicatechin | -6.1 | 1293 | -29, 20, 21 | 29, 21, 21 | Chain B: TYR140 ALA143 ARG144 SER147 LYS183 PRO184 GLN185 TYR221 TYR222 GLU249 GLY253 GLN254 PRO255 |
| Rosmarinic Acid | -5.9 | 1293 | -29, 20, 21 | 24, 24, 24 | Chain B: LEU252 GLN254 PRO255 ILE256 PHE257 PRO258 GLU268 LYS271 VAL272 HIS299 LYS303 VAL304 ARG306 |
| Quercetin | **-6.5** | 1293 | -29, 20, 21 | 29, 21, 21 | Chain B: TYR140 ALA143 ARG144 SER147 GLN185 SER219 TYR221 TYR222 GLU249 GLY253 GLN254 PRO255 |
| Myricetin | -6.3 | 1293 | -29, 20, 21 | 29, 21, 21 | Chain B: TYR140 ALA143 ARG144 SER147 PRO184 GLN185 SER219 TYR221 TYR222 GLU249 GLY253 GLN254 PRO255 |
| Metformin | **-4.3** | 1293 | -29, 20, 21 | 29, 16, 16 | Chain B: THR152 LEU153 VAL155 LEU250 LEU251 LEU252 PHE305 ARG306 PRO307 ARG308 THR309 PRO310 |

Table 7 — Lead compounds and their docking score with competitive targets

| Name | Adiponectin | α-amylase | α-glucosidase | PPARγ | GSK-3β | Targets (>standard) |
|---|---|---|---|---|---|---|
| Catechin hydrate | -6.7 | -9.1 | -7.2 | -8.0 | -5.9 | 4 |
| Epicatechin | -7.0 | -9.0 | -7.1 | -8.0 | -6.1 | 4 |
| **Rosmarinic acid** | -6.4 | -7.9 | -7.9 | -8.2 | -5.9 | **5** |
| **Quercetin** | -7.2 | -9.0 | -7.1 | -8.5 | -6.5 | **5** |
| Myricetin | -7.2 | -9.0 | -6.6 | -7.5 | -6.3 | 3 |
| Standard | **-5.9** | **-7.5** | **-6.7** | **-8.0** | **-4.3** | - |

metabolism, the ligands (three ligands were employed as standards) showed a superior excretion rate from the body, with maximal tolerance at dosages between 0.152 and 0.902 (log mg/kg/day). Parameters suggested that the chosen phytochemicals are not carcinogenic (Table 8), and all compounds resulted negatively in AMES toxicity and hepatotoxicity except reference compounds metformin and rosiglitazone. Furthermore, these elements satisfy the $LD_{50}$ and the superior absorption in the human intestinal epithelial cell line and (oral rat acute toxicity) requirements, which is more significant.

On the contrary, QSAR analysis predicts chemicals' potential biochemical interaction qualities,

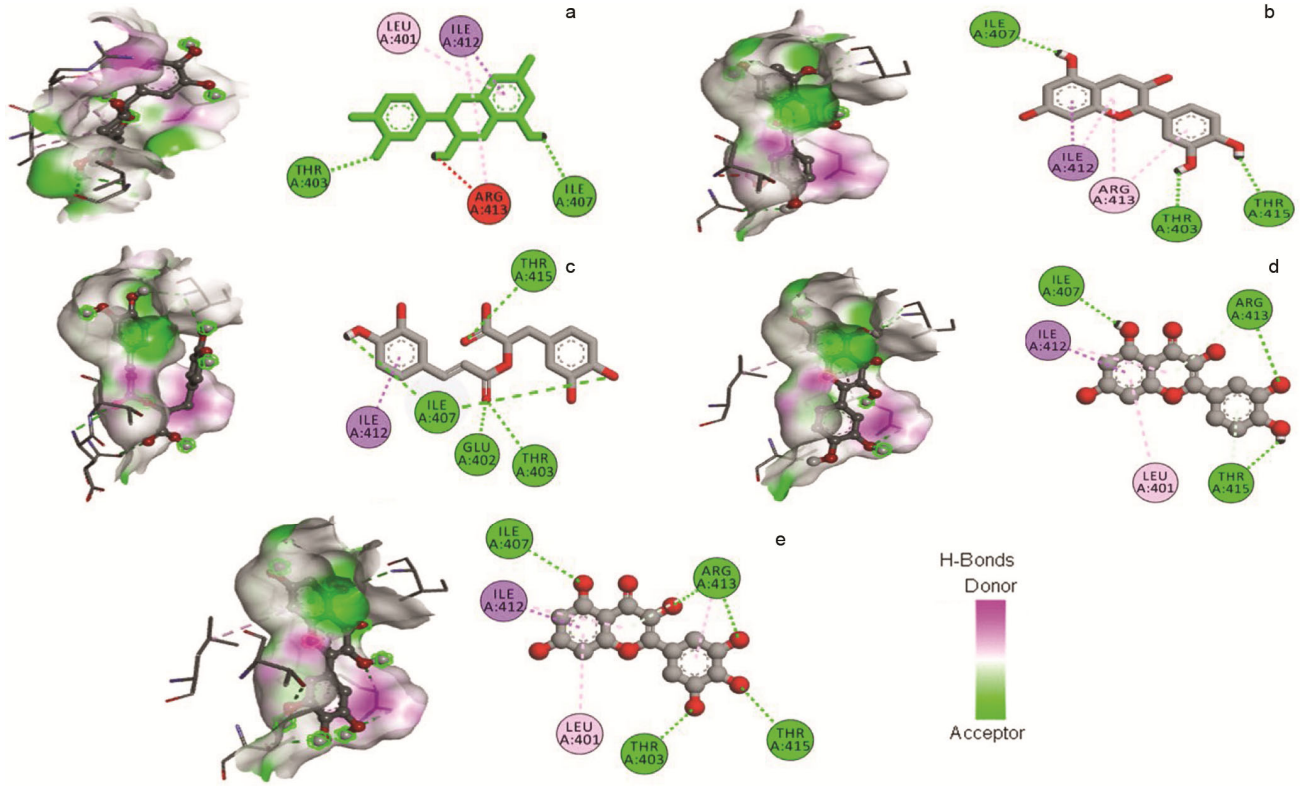


Fig. 2 — Possible docking poses of Adiponectin with a) Catechin hydrate; b) Epicatechin; c) Rosmarinic acid; d) Quercetin; and e) Myricetin.

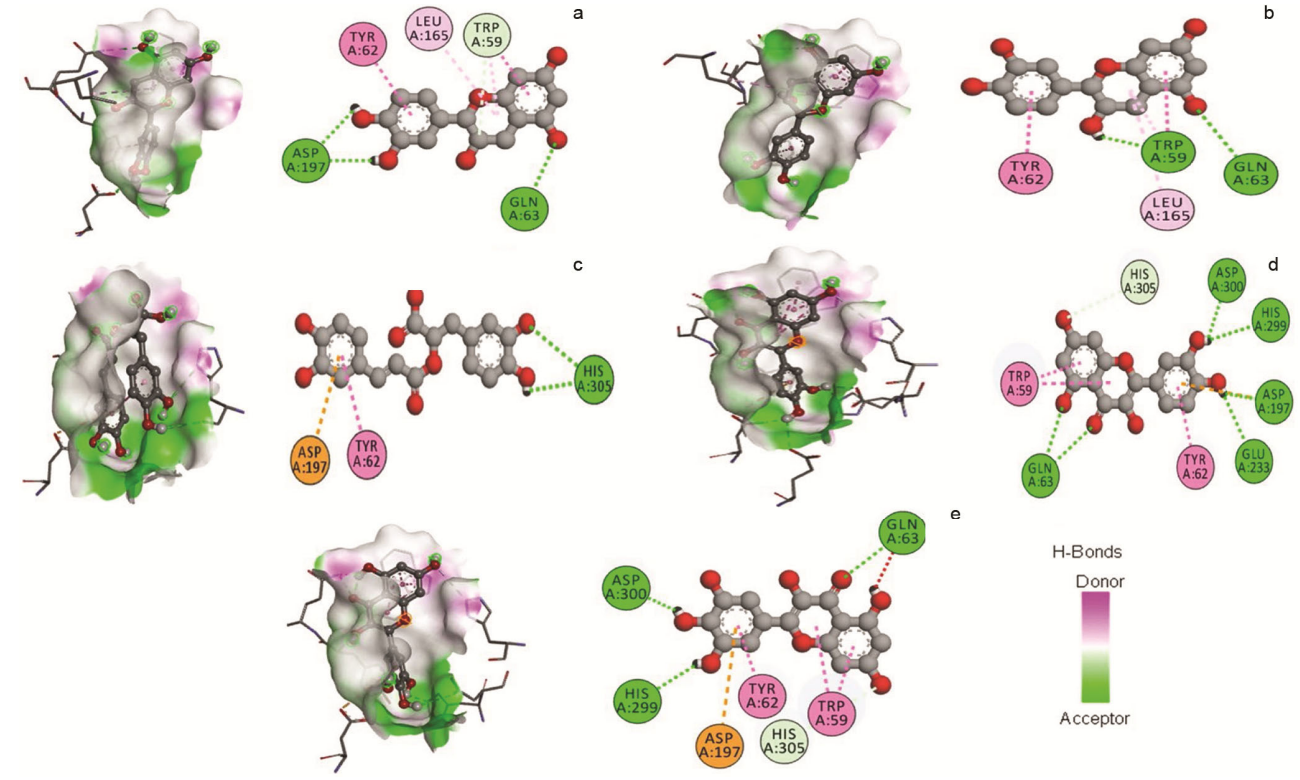


Fig. 3 — Possible docking poses of α-amylase with a) Catechin hydrate; b) Epicatechin; c) Rosmarinic acid; d) Quercetin; and e) Myricetin.

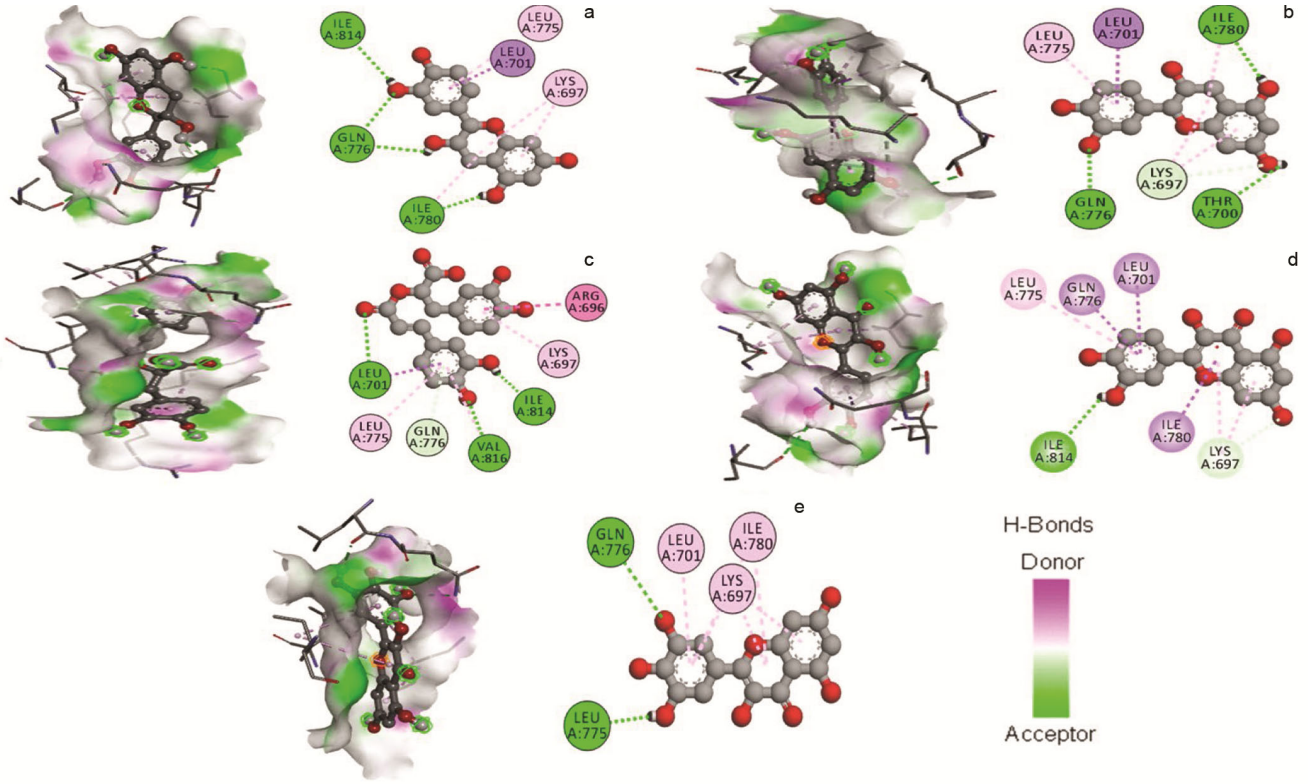


Fig. 4 — Possible docking poses of α-glucosidase with a) Catechin hydrate; b) Epicatechin; c) Rosmarinic acid; d) Quercetin; and e) Myricetin.

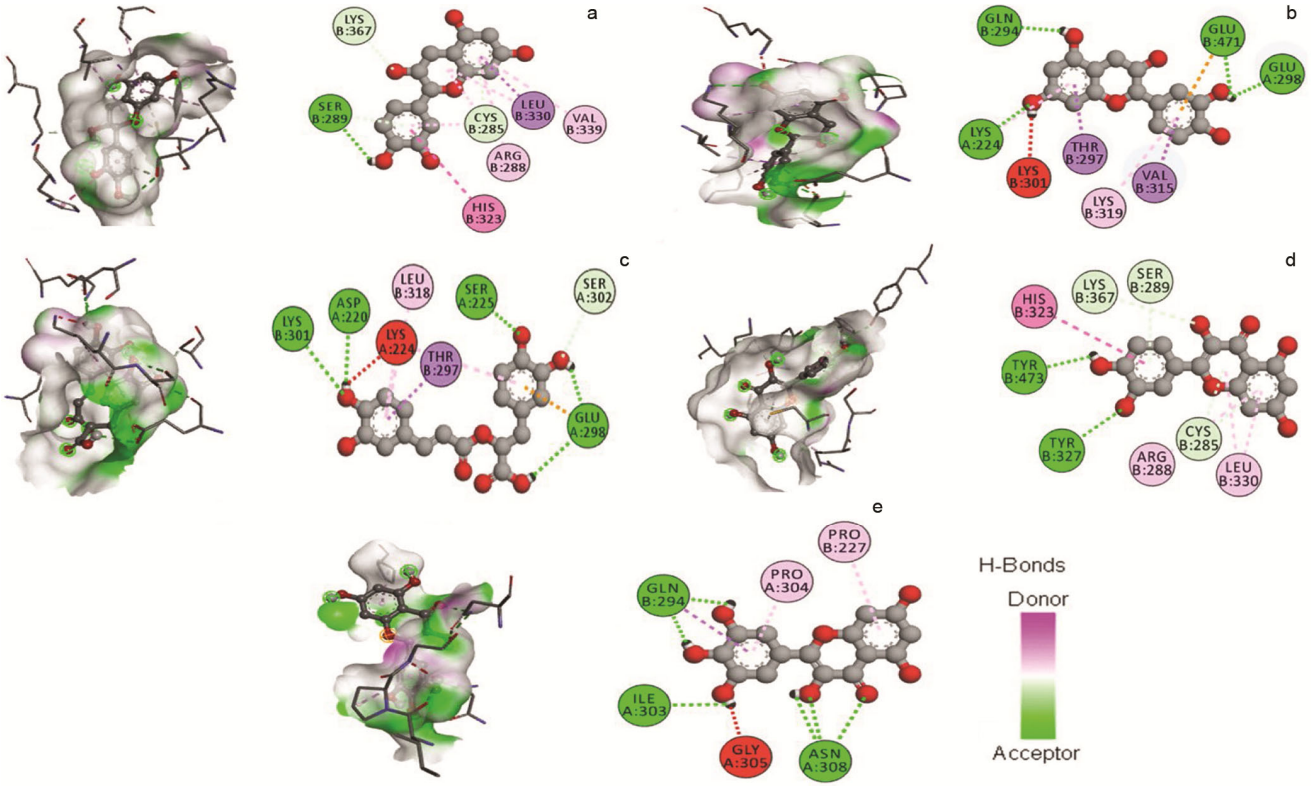


Fig. 5 — Possible docking poses of PPARγ with a) Catechin hydrate; b) Epicatechin; c) Rosmarinic acid; d) Quercetin; and e) Myricetin.

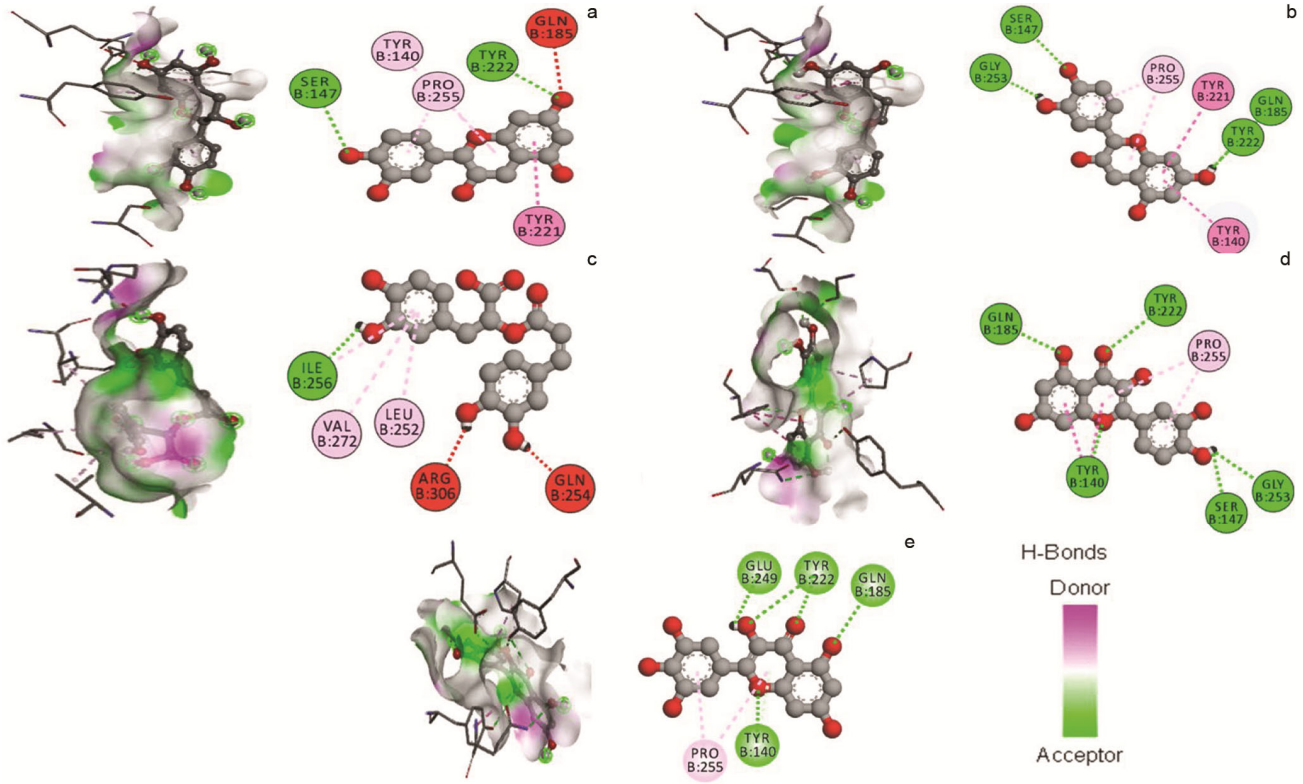


Fig.6 — Possible docking poses of GSK-3β with a) Catechin hydrate; b) Epicatechin; c) Rosmarinic acid; d) Quercetin; and e) Myricetin.

Table 8 — ADMET properties of selective ligands

| Compounds | IA | TC | LD50 | HT | AT | MTD | DL |
|---|---|---|---|---|---|---|---|
| Catechin Hydrate | 63.919 | 0.181 | 2.399 | NO | NO | 0.442 | YES |
| Epicatechin | 68.829 | 0.183 | 2.428 | NO | NO | 0.438 | YES |
| Rosmarinic Acid | 32.516 | 0.25 | 2.811 | NO | NO | 0.152 | YES |
| Quercetin | 77.207 | 0.407 | 2.471 | NO | NO | 0.499 | YES |
| Myricetin | 65.93 | 0.422 | 2.497 | NO | NO | 0.51 | YES |
| Rosiglitazone | 93.757 | 0.107 | 2.692 | YES | NO | 0.066 | YES |
| Acarbose | 4.172 | 0.428 | 2.449 | NO | NO | 0.435 | YES |
| Metformin | 59.401 | 0.1 | 2.453 | NO | YES | 0.902 | YES |

IA = Intestinal absorption (% absorbed); TC = Total clearance (log mL/min/kg); LD50 = Oral rat acute toxicity; HT = Hepatotoxicity; AT = AMES toxicity; MTD = Maximum tolerated dose for human (log mg/kg/day); NLV = No. of Lipinski's rule violations; DL = Drug-likeness (Lipinski's rule).

Table 9 — QSAR properties of selected ligands

| Compounds | Lipinski Parameters | | | | | | | |
|---|---|---|---|---|---|---|---|---|
| | M.W. | H-Bond Acceptors | H-Bond Donors | TPSA | LogPo/w | MR | RB | Lipinski Violation |
| Catechin Hydrate | 309.27 | 6 | 5 | 119.38 | 1.33 | 74.33 | 1 | 0 |
| Epicatechin | 290.20 | 6 | 5 | 110.38 | 1.33 | 74.33 | 1 | 0 |
| Rosmarinic Acid | 360.31 | 8 | 5 | 144.52 | 1.48 | 91.40 | 7 | 0 |
| Quercetin | 302.24 | 7 | 5 | 131.36 | 1.63 | 78.04 | 1 | 0 |
| Myricetin | 318.24 | 8 | 6 | 151.59 | 1.08 | 80.06 | 1 | 1 |

making it an essential step in identifying those with drug-like effects. Current research analysed the chosen ligands using the Lipinski rule of five to determine a variety of QSAR descriptors. Table 9 presents a quick summary of the outcome. The reported molecular weights of ligands ranged from 290.20-360.31Da. These values fell within the range of 500 Da or less; therefore, they were safe and effective according to Lipinski's first criteria for drug delivery. As per a second criterion, the number of hydrogen bond contributing groups should be limited to no more than five. Except for myricetin, all ligands followed this principle.

Moreover, the number of hydrogen-bond accepting groups was within 6–8, with a maximum of 10, while the logP value was in the range of 1.08–1.63, with a maximum of 5. In addition, their estimated molecular refractivity ranged from 74.33 to 91.40 $cm^3$/mol, indicating promising therapeutic potential. Accordingly, four ligands exhibited no Lipinski violations, whereas one ligand (Myricetin) broke a single rule. Total polar surface area (TPSA) values for three different ligands were found within 110.38–131.36, much below the theoretical maximum of 140, and with values over 140, two ligands, rosmarinic acid and myricetin, predicted low oral bioavailability. Finally, the QSAR prediction of the selected ligands' features confirmed their efficient physicochemical relationships to exert and endorse robust antioxidant activities as an anti-diabetic medication.

**Deformability, B-factor, and covariance analysis**

Molecular dynamics simulation ((MDS) is a valuable tool for determining the stability of protein-ligand complexes. Only Rosmarinic acid and Quercetin, the best docking complexes against five chosen targets, were considered for the MDS analysis.

The deformability of a molecule is a quantitative measure of its flexibility at each residue. The "highest peaks" that emerge from areas of excellent deformability are the most obvious manifestation of this phenomenon. Fig. 7 (a, d, g, j, m) and Fig. 8 (a, d, g, j, m) depicted the deformability graphs of the Rosmarnic acid and Quercetin complexes, respectively. However, Rosmarinic and Quercetin complexes had peaks of around 1.0 deformability index, indicating high flexibility[42]. We use normal mode analysis (NMA) on the PDB structure to get the B-factor and multiply the NMA mobility by $8pi^2$. The B-factor analysis also provides an estimated root-mean-square (RMS) value. Nevertheless, Rosmarinic acid complexes, on the other hand, were substantially better than quercetin complexes illustrated in Fig. 7 (b, e, h, k, n) and 8 (b, e, h, k, n). The covariance matrix reveals the correlation between the complex's residues; the stronger the correlation, the better the complex. A high degree of correlation is shown in red, a lack of correlation in white, and anticorrelation in blue. These findings were shown graphically in Fig. 7 (c, f, i, l,o) and Fig. 8 (c, f, i, l,o).

Based on the molecular dynamics analysis, it was clear that our selected complexes exhibited a high degree of deformability around the flexible hinge regions. The mobility profile and relative amplitude of atomic displacements close to the equilibrium conformation were revealed by the NMA B-factor. The covariance matrix also showed the relationships between the residues (red for correlated, white for uncorrelated, and blue for anti-correlated) in a graphical manner.

**RMSF investigation**

RMSF is a measure used to quantify a molecule's flexibility or dynamic behaviour in molecular dynamics simulations or structural biology studies. It gives crucial information regarding atom or residue flexibility in biomolecular structures.

The RMSF of atomic positions in a protein structure provides insights into the flexibility of different regions or residues. Higher RMSF values indicate more mobile or flexible regions, while lower RMSF values indicate more rigid or constrained areas. This information is crucial for understanding the functional properties of proteins, such as their binding capabilities, enzymatic activity, or allosteric regulation. RMSF plot for the selective complexes is shown in Fig. 9–13.

The RMSF pattern of the selective ligands (rosmarinic acid, quercetin, and rosiglitazone) against adiponectin was projected to be quite similar, illustrated in Fig. 9. However, as compared to conventional rosiglitazone, quercetin, and rosmarinic acid exhibited the maximum fluctuations at residues 248 (6.55 Å) and 386 (4.766 Å), respectively. In addition, in the case of α-amylase, quercetin exhibited greater fluctuations at residue 143 (6.05 Å) than acarbose, but rosmarinic acid showed similar fluctuations compared to acarbose (Fig. 10). Additionally, as compared to acarbose, rosmarinic acid exhibited the most significant shifts at residue 894 (7.462 Å) and minimal fluctuations at residue 599 (0.046 Å) (Fig. 11) against α-glucosidase. At the same time, acarbose and quercetin had the same RMSF trend. Further, Fig. 12 depicts the RMSF profile of all selective ligands against PPAR, which was reasonably comparable to that of rosiglitazone. Lastly, in the case of GSK3β, all of the chosen ligands displayed a similar pattern in their RMSF traits; however,rosmarinic acid showed more significant fluctuations at residue level 289 (8.299 Å) than metformin (Fig. 13).

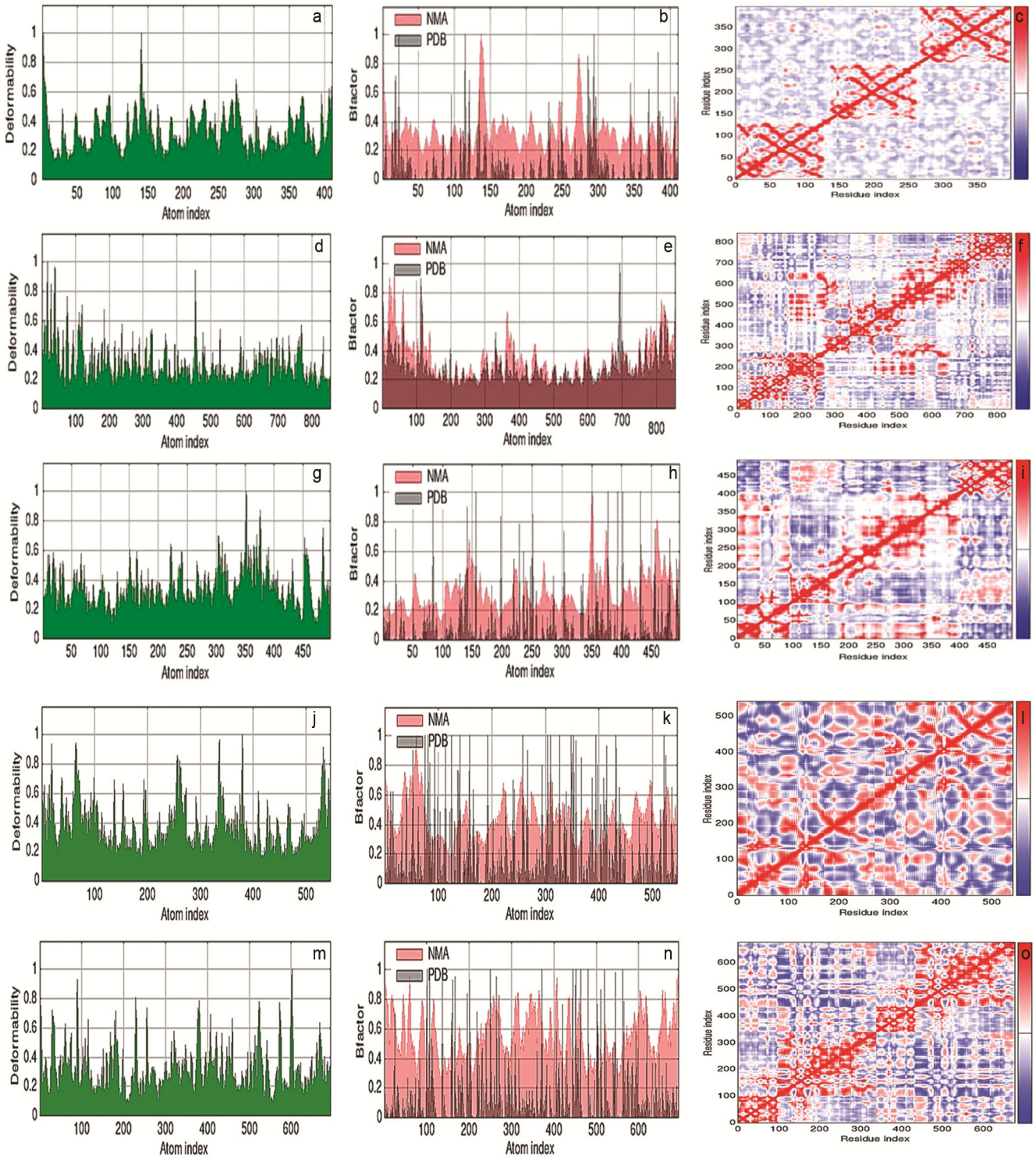


Fig. 7 —Rosmarinic Acid_Adiponectin, a) Deformability; b) B-factor; c) Covariance analysis; Rosmarinic Acid_α-amylase; d) Deformability; e) B-factor; f) Covariance analysis; Rosmarinic Acid_α-glucosidase; g) Deformability; h) B-factor; i) Covariance analysis; RosmarinicAcid_PPARγ j) Deformability; k) B-factor; l) Covariance analysis; Rosmarinic Acid_GSK-3β; m) Deformability; n) B-factor; and o) Covariance analysis, respectively.

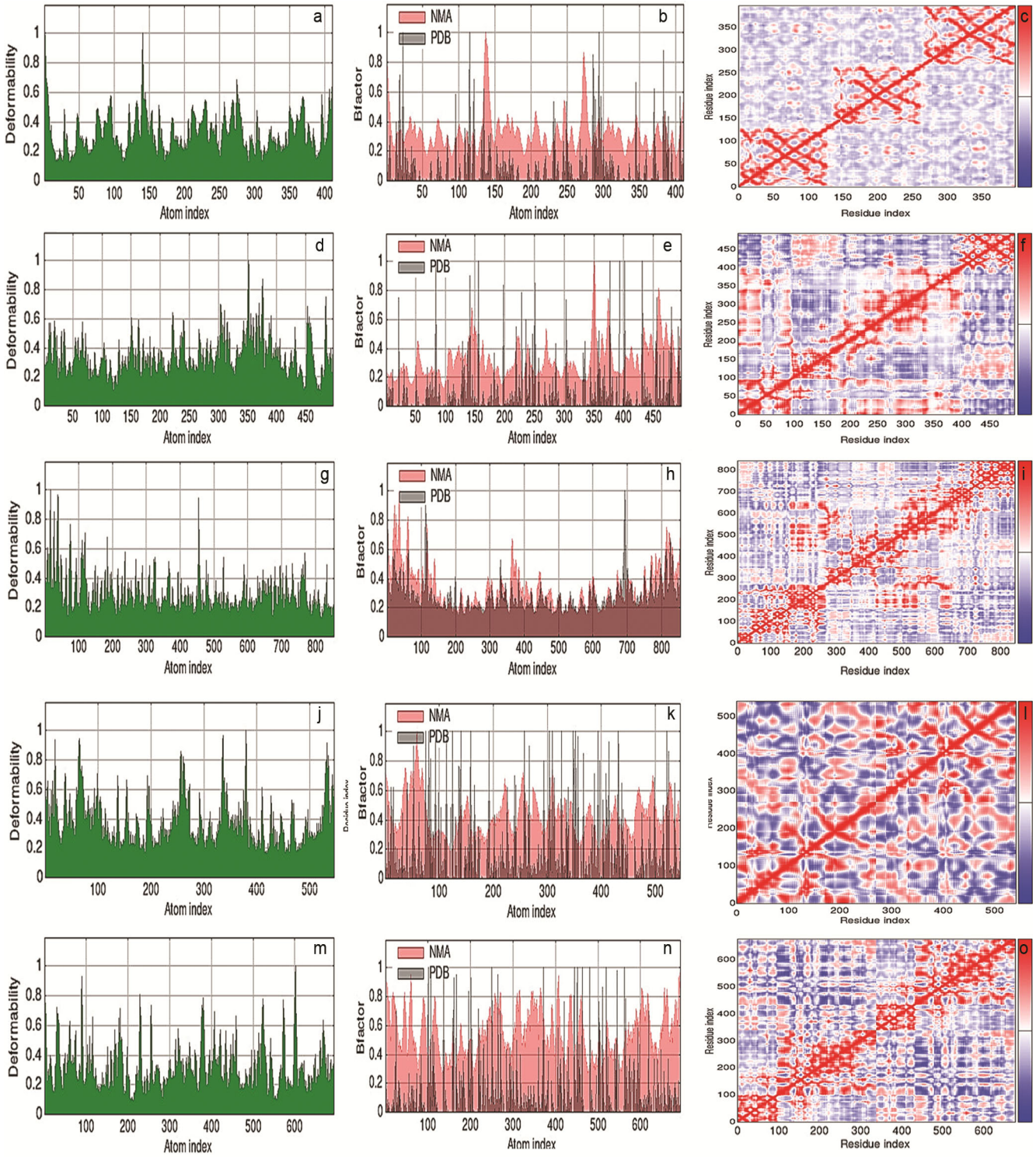


Fig. 8 — Quercetin_Adiponectin, a) Deformability; b) B-factor; c) Covariance analysis; Quercetin_α-amylase; d) Deformability; e) B-factor; f) Covariance analysis; Quercetin_α-glucosidase; g) Deformability; h) B-factor; and i) Covariance analysis, Quercetin_PPARγ, j) Deformability; k) B-factor; l) Covariance analysis; Quercetin_GSK-3β; m) Deformability; n) B-factor; and o) Covariance analysis, respectively.

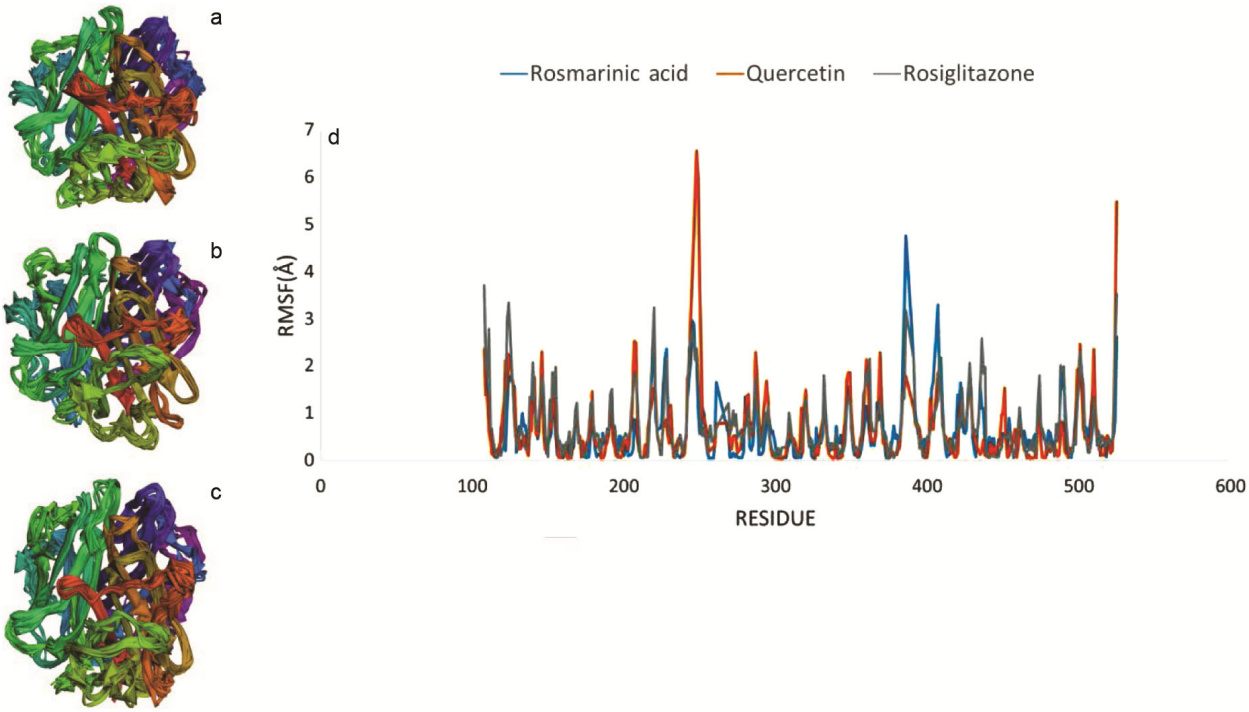


Fig. 9 — Multimodel superimposed simulated structure. a) Rosmarinic acid; b) Quercetin; c) Rosiglitazone showing; and d) RMSF profile of against adiponectin.

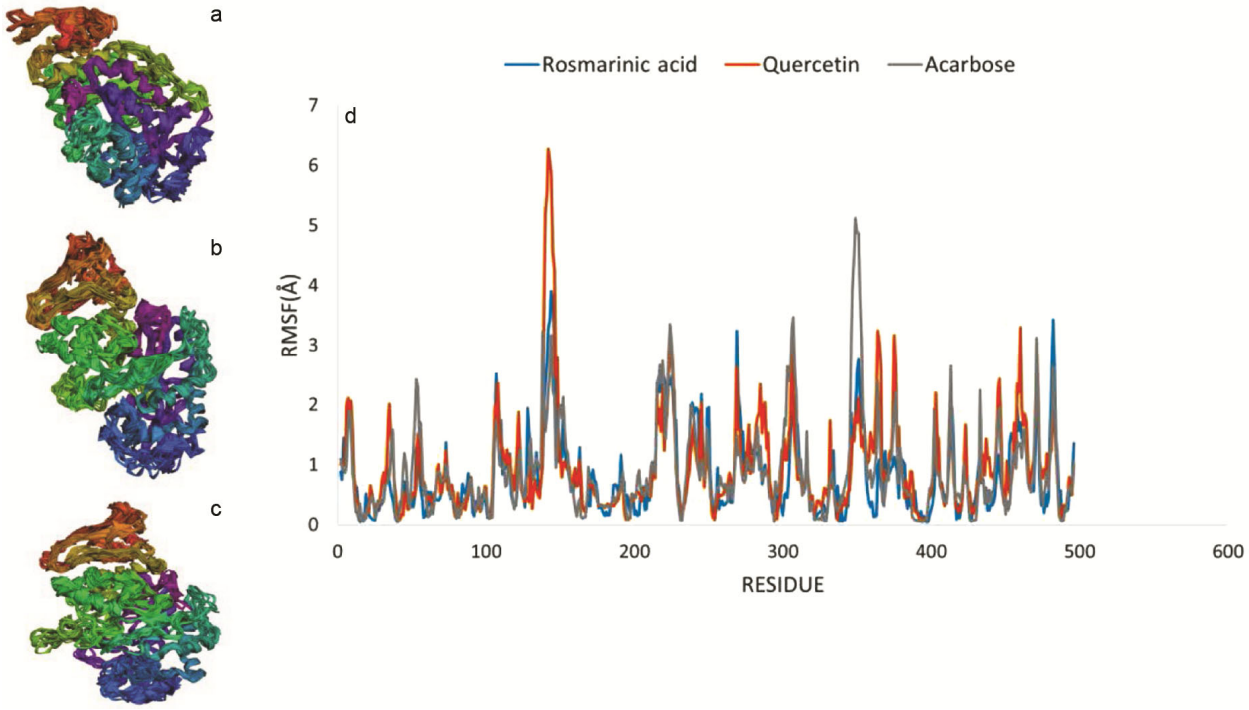


Fig. 10 — Multimodel superimposed simulated structure. a) Rosmarinic acid; b) Quercetin; c) Rosiglitazone showing; and d) RMSF profile against α-amylase.

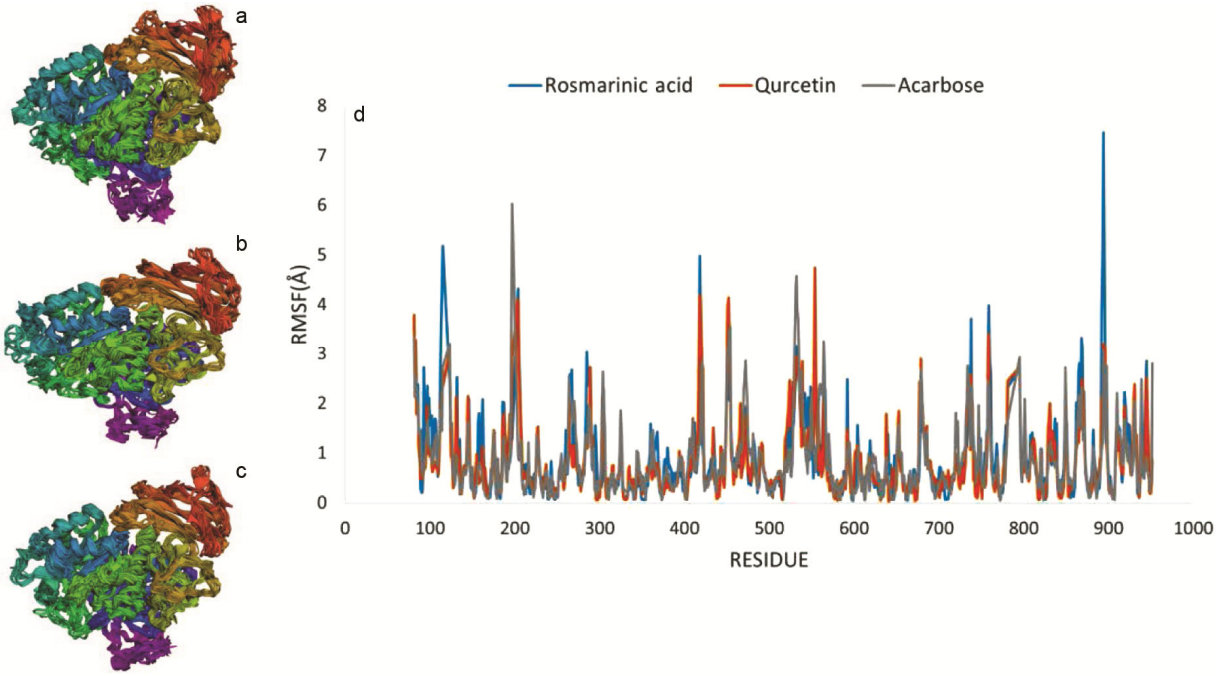


Fig. 11 — Multimodel superimposed simulated structure. a) Rosmarinic acid; b) Quercetin; c) Rosiglitazone showing; and d) RMSF profile against α-glucosidase.

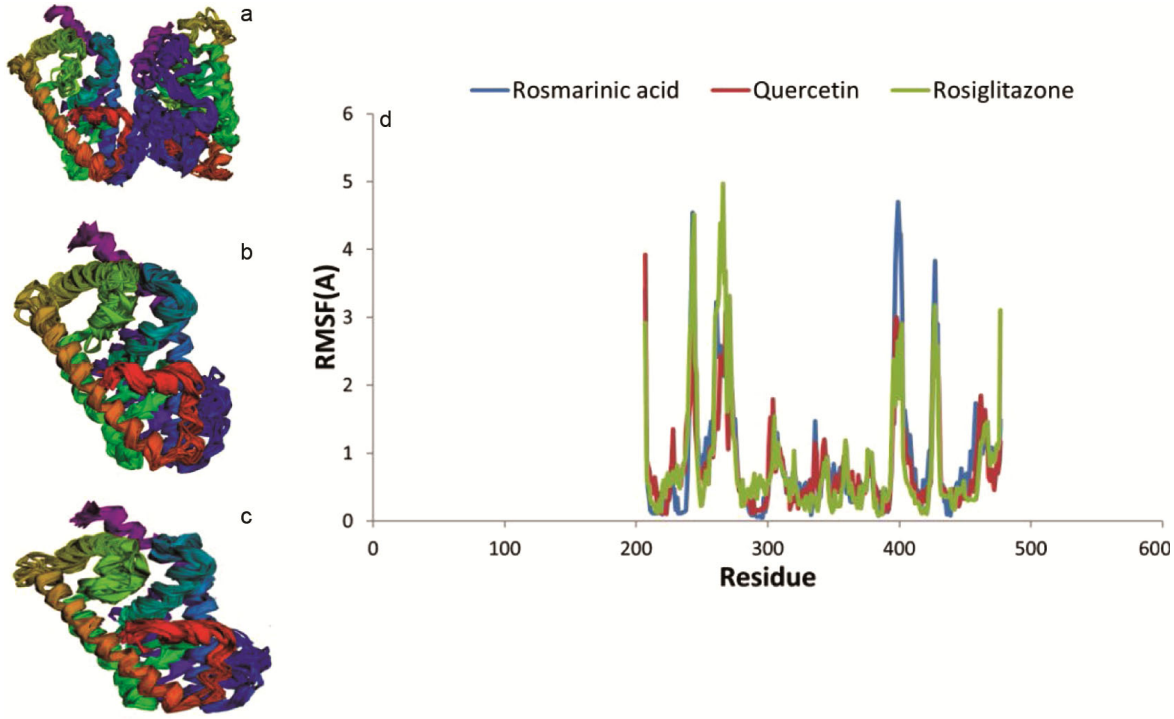


Fig. 12 — Multimodel superimposed simulated structure. a) Rosmarinic acid; b) Quercetin; c) Rosiglitazone showing; and d) RMSF profile against PPARγ.

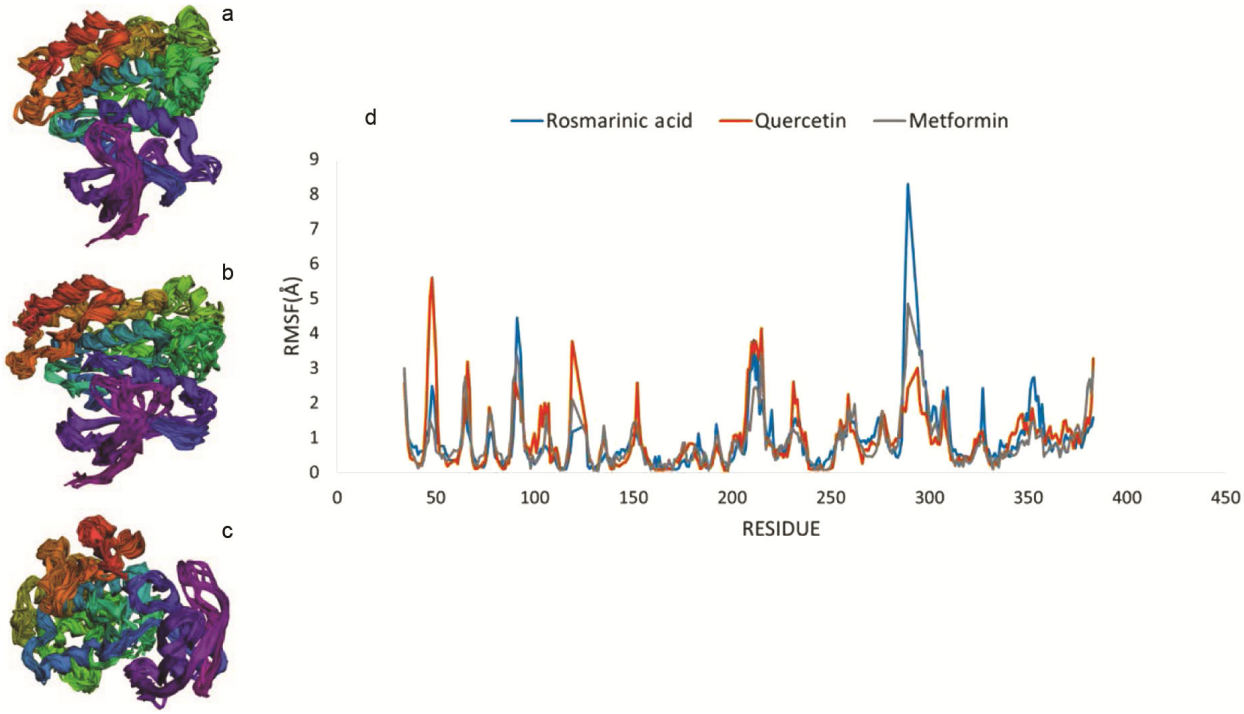


Fig. 13 — Multimodel superimposed simulated structure. a) Rosmarinic acid; b) Quercetin; c) Rosiglitazone showing; and d) RMSF profile against GSK3β.

## Conclusion

In the present study, we investigated five bioactive phytochemicals identified from the *Z. roseum* plant in search of potential anti-diabetic actions. Five phytochemicals passed the ADMET and QSAR score assessments; however, only two, rosmarinic acid and quercetin, showed significant binding with adiponectin (-6.4 and -7.2 kcal/mol), α-amylase (-7.9 and -9.0 kcal/mol), α-glucosidase (-7.9 and -7.1 kcal/mol), peroxisome proliferator-activated receptor (PPARγ) (-8.2 and -8.5 kcal/mol), and glycogen synthase kinase-3β (GSK-3β) (-5.9 and -6.5 kcal/mol). Moreover, the dynamic simulation study also demonstrated more stability of chosen protein-ligand complexes. Therefore, it is reasonable to assume that our ligand molecules hold the key to cure diabetes. More *in-vitro* and *in vivo* investigations may be needed to determine efficacy as well as suggest the precise mechanism.

## Conflict of interest

The authors declare no conflict of interest.

## References

1 Koyutürk M, Özsoy-Saçan Ö, Bolkent Ş and Yanardağ R, Effect of glurenorm on immunohistochemical changes in pancreatic β cells of rats in experimental diabetes, *Indian J Exp Biol*, 2005, **43**(03), 268-271.

2 Burke J, Williams K, Narayan K V, Leibson C, Haffner S M, *et al.*, A population perspective on diabetes prevention: Whom should we target for preventing weight gain?, *Diabetes Care*, 2003, **26**(7), 1999-2004, doi: 10.2337/diacare.26.7.1999.

3 Group I D F, Update of mortality attributable to diabetes for the IDF Diabetes Atlas: Estimates for the year2013, *Diabetes Res Clin Pract*, 2015, **109**(3), 461-465, doi: 10.1016/j.diabres.2015.05.037.

4 Boon N A, Davidson's principles and practice of medicine, 20th edn, (Churchill Livingstone), 2006.

5 Reynolds L J, Credeur D P, Manrique C, Padilla J, Fadel P J, *et al.*, Obesity, type 2 diabetes, and impaired insulin-stimulated blood flow: Role of skeletal muscle NO synthase and endothelin-1, *J Appl Physiol*, 2017, **122**(1), 38-47, doi: 10.1152/japplphysiol.00286.2016.

6 Piedrola G, Novo E, Escobar F and Garcia-Robles R, White blood cell count and insulin resistance in patients with coronary artery disease, *Ann Endocrinol*, 2001, **63**, 7-10.

7 Yaryura-Tobias J A, Pinto A and Neziroglu F, Anorexia nervosa, diabetes mellitus, brain atrophy, and fatty liver, *Int J Eat Disord*, 2001, **30**(3), 350-353, doi: 10.1002/eat.1096.

8 Anuradha K, Hota D and Pandhi P, Investigation of central mechanism of insulin induced hypoglycaemic convulsions in mice, *Indian J Exp Biol*, 2004, **42**(04), 368-372.

9 Olawale F, Aninye I, Ajaja U and Nwozo S, Long-term hyperglycemia impairs hormonal balance and induces oxidative damage in ovaries of streptozotocin-induced diabetic wistar rat, *Niger J Physiol Sci*, 2020, **35**(1), 46-51.

10 Pitchai D and Manikkam R, Hypoglycemic and insulin mimetic impact of catechin isolated from Cassia fistula: A substantiate *in silico* approach through docking analysis, *Med*

*Chem Res*, 2011, **21**(9), 2238-2250, doi: 10.1007/s00044-011-9722-1.

11 Kavishankar G, Lakshmidevi N, Murthy S M, Prakash H and Niranjana S, Diabetes and medicinal plants-A review, *Int J Pharm Biomed Sci*, 2011, **2**(3), 65-80.

12 Kooti W, Farokhipour M, Asadzadeh Z, Ashtary-Larky D and Asadi-Samani M, The role of medicinal plants in the treatment of diabetes: A systematic review, *Electron Physician*, 2016, **8**(1), 1832, doi: 10.19082/1832.

13 Arumugam G, Manjula P and Paari N, A review: Anti diabetic medicinal plants used for diabetes mellitus, *J Acute Dis*, 2013, **2**(3), 196-200, doi: 10.1016/S2221-6189(13)60126-2.

14 Olawale F, Olofinsan K, Iwaloye O and Ologuntere T, Phytochemicals from Nigerian medicinal plants modulate therapeutically-relevant diabetes targets: Insight from computational direction, *Adv Trad Med*, 2021, **22**, 1-15, doi: 10.1007/s13596-021-00598-z.

15 Amanat M, Reza M S, Shuvo M, Ahmed K, Hossain H, *et al.*, *Zingiber roseum* Rosc. rhizome: A rich source of hepatoprotective polyphenols, *Biomed Pharmacother*, 2021, **139**, 111673, doi: 10.1016/j.biopha.2021.111673.

16 Prakash O, Kasana V, Pant A, Zafar A, Hore S, *et al.*, Phytochemical composition of essential oil from seeds of *Zingiber roseum* Rosc. and its antispasmodic activity in rat duodenum, *J Ethnopharmacol*, 2006, **106**(3), 344-347, doi: 10.1016/j.jep.2006.01.016.

17 Amanat M, Tawhid M and Shahid A F M, Anthelmintic activity of *Zingiber roseum* rhizomes against Pheretima posthuma: *In vitro* and *in silico* approach, *Int J Sci Res Chem*, 2022, **7**(1), 1-15, doi: 10.5281/zenodo.7303136.

18 Benavente-García O, Castillo J, Marin F R, Ortuño A and Del J, Uses and properties of citrus flavonoids, *J Agric Food Chem*, 1997, **45**(12), 4505-4515, doi: 10.1021/jf970373s.

19 Manach C, Mazur A and Scalbert A, Polyphenols and prevention of cardiovascular diseases, *Curr Opin Lipidol*, 2005, **16**(1), 77-84.

20 Middleton E, Kandaswami C and Theoharides T, The effects of plant flavonoids on mammalian cells: Implications for inflammation, heart disease, and cancer, *Pharmacol Rev*, 2000, **52**(4), 673-751.

21 Puupponen-Pimiä R, Nohynek L, Meier C, Kähkönen M, Heinonen M, *et al.*, Antimicrobial properties of phenolic compounds from berries, *J Appl Microbiol*, 2001, **90**(4), 494-507, doi: 10.1046/j.1365-2672.2001.01271.x.

22 Cotelle N, Role of flavonoids in oxidative stress, *Curr Top Med Chem*, 2001, **1(**6), 569-590, doi: 10.2174/1568026013394750.

23 Vazhappilly C G, Ansari S A, Al-Jaleeli R, Al-Azawi A M, Ramadan W S, *et al.*, Role of flavonoids in thrombotic, cardiovascular, and inflammatory diseases, *Inflammopharmacology*, 2019, **27**, 863-869, doi: 10.1007/s10787-019-00612-6.

24 Zanoaga O, Braicu C, Jurj A, Rusu A, Buiga R, *et al.*, Progress in research on the role of flavonoids in lung cancer, *Int J Mol Sci*, 2019, **20**(17), 4291, doi: 10.3390/ijms20174291.

25 Shukla R, Pandey V, Vadnere G P and Lodhi S, Role of flavonoids in management of inflammatory disorders, in *Bioactive Food as Dietary Interventions for Arthritis and Related Inflammatory Diseases*, (Elsevier), 2019, 293-322, doi: 10.1016/B978-0-12-813820-5.00018-0.

26 Testa R, Bonfigli A R, Genovese S, De Nigris V and Ceriello A, The possible role of flavonoids in the prevention of diabetic complications, *Nutrients*, 2016, **8**(5), 310, doi: 10.3390/nu8050310.

27 Kawano J and Arora R, The role of adiponectin in obesity, diabetes, and cardiovascular disease, *J Cardiometabolic Syndr*, 2009, **4**(1), 44-49, doi: 10.1111/j.1559-4572.2008.00030.x.

28 Chakraborti C, Role of adiponectin and some other factors linking type 2 diabetes mellitus and obesity, *World J Diabetes*, 2015, **6**(15), 1296, doi:10.4239/wjd.v6.i15.1296.

29 Hossain U, Das A K, Ghosh S and Sil P, An overview on the role of bioactive α-glucosidase inhibitors in ameliorating diabetic complications, *Food Chem Toxicol*, 2020, **145**, 111738, doi: 10.1016/j.fct.2020.111738.

30 Unnikrishnan P, Suthindhiran K and Jayasri M, Alpha-amylase inhibition and antioxidant activity of marine green algae and its possible role in diabetes management, *Pharmacogn Mag*, 2015, **11**(Suppl 4), S511, doi: 10.4103/0973-1296.172954.

31 Wulan D R, Utomo E P and Mahdi C, Antidiabetic activity of *Ruellia tuberosa* L., role of α-amylase inhibitor: *in silico*, *in vitro*, and *in vivo* approaches, *Biochem Res Int*, 2015, **2015**, 1-9, doi: 10.1155/2015/349261.

32 Khadayat K, Marasini B P, Gautam H, Ghaju S and Parajuli N, Evaluation of the alpha-amylase inhibitory activity of Nepalese medicinal plants used in the treatment of diabetes mellitus, *Clin Phytoscience*, 2020, **6**(1), 1-8, doi: 10.1186/s40816-020-00179-8.

33 Kaur N, Kumar V, Nayak S K, Wadhwa P, Kaur P, *et al.*, Alpha-amylase as molecular target for treatment of diabetes mellitus: A comprehensive review, *Chem Biol Drug Des*, 2021, **98**(4), 539-560, doi: 10.1111/cbdd.13909.

34 Rangwala S M and Lazar M A, Peroxisome proliferator-activated receptor γ in diabetes and metabolism, *Trends Pharmacol Sci*, 2004, **25**(6), 331-336, doi: 10.1016/j.tips.2004.03.012.

35 Bermudez V, Finol F, Parra N, Parra M, Pérez A, *et al.*, PPAR-γ agonists and their role in type 2 diabetes mellitus management, *Am J Ther*, 2010, **17**(3), 274-283, doi: 10.1097/MJT.0b013e3181c08081.

36 Natarajan A, Sugumar S, Bitragunta S and Balasubramanyan N J, Molecular docking studies of (4 Z, 12 Z)-cyclopentadeca-4, 12-dienone from Grewia hirsuta with some targets related to type 2 diabetes, *BMC Complement Altern Med*, 2015, **15**, 1-8, doi: 10.1186/s12906-015-0588-5.

37 Herowati R and Widodo G P, Molecular docking studies of chemical constituents of *Tinospora cordifolia* on glycogen phosphorylase, *Procedia Chem*, 2014, **13**, 63-68, doi: 10.1016/j.proche.2014.12.007.

38 Hassan N M, Alhossary A A, Mu Y and Kwoh C, Protein-ligand blind docking using QuickVina-W with inter-process spatio-temporal integration, *Sci Rep*, 2017, **7**(1), 15451, doi: 10.1038/s41598-017-15571-7.

39 Dey D, Paul P K, Azad S, Mazid M F, Khan A M, *et al.*, Molecular optimization, docking, and dynamic simulation profiling of selective aromatic phytochemical ligands in blocking the SARS-CoV-2 S protein attachment to ACE2 receptor: An *in silico* approach of targeted drug

designing, *J Adv Vet Anim Res*, 2021, **8**(1), 24, doi: 10.5455/javar.2021.h481.

40 Marwaha A, Goel R and Mahajan M, PASS-predicted design, synthesis and biological evaluation of cyclic nitrones as nootropics, *Bioorg Med Chem*, 2007, **17**(18), 5251-5255, doi: 10.1016/j.bmcl.2007.06.071.

41 Amanat M, Daula A S U and Islam F, Potential usage of Zerumbone to suppress inflammation: An *in silico* study, *Am J Sci Med Res*, 2022, **8**(2), 1-11.

42 Qazi S, Das S, Khuntia B K, Sharma V, Sharma S, *et al.*, *In silico* molecular docking and molecular dynamic simulation analysis of phytochemicals from indian foods as potential inhibitors of SARS-CoV-2 RdRp and 3CLpro, *Nat Prod Commun*, 2021, **16**(9), doi: 10.1177/1934578X211056753.

43 Kurcinski M, Oleniecki T, Ciemny M P, Kuriata A, Kolinski A, *et al.*, CABS-flex standalone: A simulation environment for fast modeling of protein flexibility, *Bioinformatics*, 2019, **35**(4), 694-695, doi: 10.1093/bioinformatics/bty685.

44 Oprea T I and Matter H, Integrating virtual screening in lead discovery, *Curr Opin Chem Biol*, 2004, **8**(4), 349-358, doi: 10.1016/j.cbpa.2004.06.008.